Deformation and Recrystallization Textures in Metals and Quartz

R. W. Cahn

Phil. Trans. R. Soc. Lond. A 1978 **288**, 159-176
doi: 10.1098/rsta.1978.0011

Phil. Trans. R. Soc. Lond. A. **288**, 159–176 (1978)   [159]
Printed in Great Britain

Deformation and recrystallization textures in metals and quartz

By R. W. Cahn
School of Engineering and Applied Sciences, University of Sussex, Brighton

The nature and graphical representation of preferred orientations, or textures, in polycrystalline assemblies is outlined. The genesis of textures during plastic deformation of metals is examined in terms of single crystal behaviour, with special reference to the formation of deformation bands, and the influence of pre-existing texture on subsequent plastic deformation (including creep) is exemplified. Next, the nature and origin of textures formed by annealing after plastic deformation are analysed and the relative rôles of oriented nucleation and oriented growth assessed.

A different kind of texture in stressed polycrystalline quartz is formed as a consequence of Dauphiné twinning. This form of twinning is explained in some detail and the origin of the textures explained in terms of the driving force that brings about Dauphiné twinning; these driving forces are compared with those that determine recrystallization in metals.

1. Introduction

A *texture* (metallurgy) or *fabric* (geology) represents a non-random distribution of the orientations of the constituent crystal grains in a polycrystalline aggregate, which may be a drawn wire, rolled sheet, cast ingot, electroplated layer, a compressed or sheared mass of rock or a rock cylinder deformed in the laboratory under hydrostatic constraint. The texture is defined relative to an identifiable geometrical feature, such as the wire axis or the sheet normal and rolling direction. A *wire texture* has rotational symmetry about the wire axis and can be referred to that axis alone, whereas a *rolling texture*, which does not have rotational degeneracy, needs the *two* cited vectors to define it completely. Ingot and electroplated textures resemble wire textures.

Textures have hitherto been displayed in *pole figures*. These are stereographic projections of a specified crystal form, generally $\{100\}$ or $\{111\}$ in the case of metals of cubic symmetry, shown in terms of contours of population density. Figure 1, which refers to rolled copper, is an example. The metallurgical grade of copper has to be specified because the texture is sensitive to minor impurities. Figure 1 also contains the positions of several ideal textures, each of which in effect represents the orientation of a single crystal in simple crystallographic relation to the defining vectors. Thus $(112)\ [\bar{1}\bar{1}1]$ denotes (112) parallel to the rolling plane and $[\bar{1}\bar{1}1]$ parallel to the rolling direction. Metallurgical textures are commonly denoted in terms of ideal textures, though actual textures are scattered as shown in figure 1, commonly clustering about more than one ideal texture (Kalland & Davies 1972) but sometimes, as in the 'cube texture' of copper, $(100)\ [001]$, about one ideal texture only.

Metallurgical textures can in practice only be determined by X-ray diffraction (unlike the geologist's recourse to polarized light and the universal stage). This task was formerly achieved photographically, but now it is always done with the aid of a specially constructed X-ray counter diffractometer, and the process can be largely automated. A pole figure such as figure 1 determined in this way has a series of numbered contours representing multiples of the count corresponding to a random orientation distribution. An alternative form is the *inverse pole* *figure*, in which a unit triangle of the crystal is displayed in standard orientation and the distribution of a vector such as the rolling direction is shown by means of contours. Figure 10, below, is an instance of this.

Neither form of pole figure shows complete information about a real texture. In principle, if there are 10000 grains, a {100} pole figure could display 30000 poles, serially numbered, so that each grain can be individually identified. This could be done – if anyone had the patience – by a geologist using the universal stage and polarized light with a transparent, optically anisotropic mineral, or by a metallurgist using the Kossel X-ray technique or selected area electron diffraction on a thin foil. A half-way approach to this is to construct an *orientation distribution* (Bunge 1965, 1969; Roe 1965). Each grain requires 3 angles to define its position precisely, whereas an ordinary pole figure embodies 2 angles, i.e. those defining a particular crystal vector. Bunge and Roe invented a three-dimensional plot which can be displayed in serial sections, to define the full orientation distribution of a population of grains. Such a plot can be constructed, without the labour of orientating thousands of individual grains, by first constructing several pole figures for distinct {*hkl*} and using those to compute the orientation function by an iterative method. The more such pole figures that are employed as input data, the better is the angular resolution of the resultant function. This is analogous to the improvement

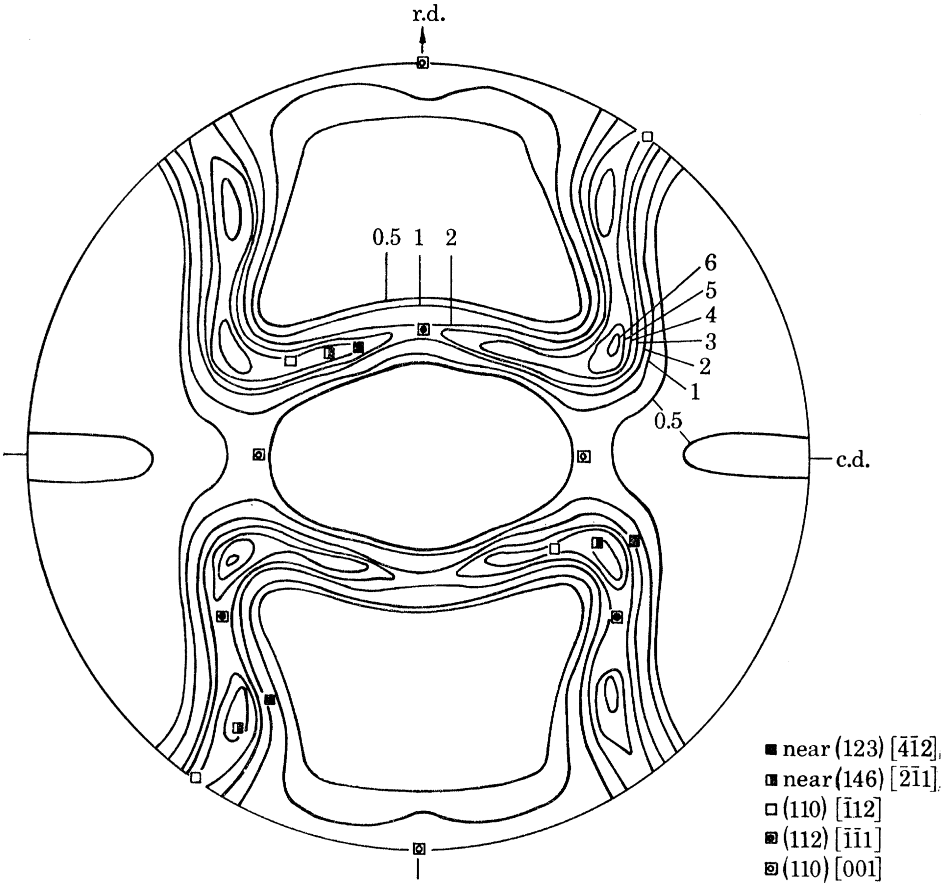

FIGURE 1. {100} pole figure of electrolytic copper rolled 96.6 % at 25 °C. Density contour of unity corresponds to randomness. r.d. and c.d. are rolling direction and cross direction, respectively, in the rolling plane. Five ideal textures are indicated. (Hu & Goodman 1963.)

of the spatial resolution of a crystal structure determination when more structure factors are included in the Fourier summations. The detailed information contained in an orientation function greatly eases the rigorous testing of theories of texture formation. The details are too involved for this review; good illustrations of the use of these functions can be found in papers by Bunge (1969) and by Dillamore & Katoh (1974).

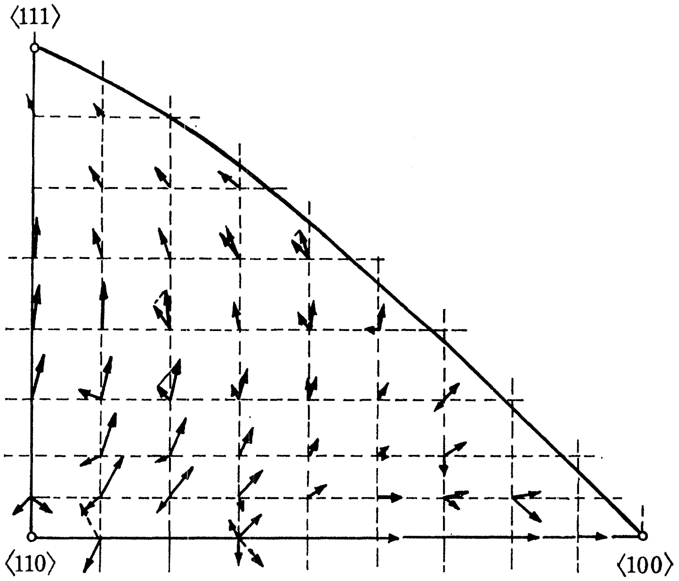

Figure 2. Lattice rotation for axisymmetric tension determined by Taylor (1934) for {110}⟨1$\bar{1}$0⟩ slip in a face-centred cubic metal, for various initial orientations. 2.37 % strain.

The enormous volume of labour which has been expended on textures of metals and alloys (Grewen & Wassermann 1962; Davies, Dillamore, Hudd & Kalland 1975) is directly due to the influence of textures on mechanical and magnetic behaviour. For many industrial purposes it is important to prevent the formation of textures altogether (thus, uranium fuel rods for certain types of nuclear reactor must be randomly orientated if catastrophic distortion in service is to be avoided), but for some major applications, such as deep drawing and the production of transformer laminations, a pronounced texture is a necessity.

2. Deformation textures

In a book which has had lasting influence and is still frequently cited, Schmid & Boas (1935) showed how the orientation of a metal rod consisting of a single grain alters when it is plastically stretched. Typically only one slip† system is active. The operative slip *direction* rotates into the rod axis. Correspondingly, a monocrystalline cylinder on compression tends to align the operative slip *plane* normal to the acting stress. As between crystallographically equivalent slip systems, that which is most highly stressed in shear is found to operate.

On the naïve view that an assembly of separate crystal grains behaves as though the grains were independent, any consistent form of plastic deformation should evidently generate a texture. In fact, the interconnected nature of the grains requires slip on multiple systems. Taylor, in a classic study (1934), showed that any one grain requires the uniform operation of at

---

† The mineralogist's term is 'translation glide'.

least 5 independent systems to achieve an arbitrary imposed strain; 'independent' here is a rather subtle concept which places restrictions on shared slip directions or planes. Taylor introduced a criterion of minimum work: that combination of 5 systems will function which minimizes $M = \Sigma\gamma_j/\epsilon$. Here M is the *Taylor factor*, γ_j is the shear in the jth slip system and ϵ is the macroscopic tensile or compressive strain. On this basis, Taylor was able to show how grains of different initial orientations, relative to the externally imposed stress, reorientated in different ways. Figure 2 is a version of his original stereogram for the tensile case, and shows his computed rotations for different starting orientations of a face-centred cubic polycrystal. Where more than one arrow appears, two or more sets of 5 slip systems are equally favoured. It is clear that orientations tend to polarize into two end-positions, with either $\langle 111\rangle$ or $\langle 100\rangle$ parallel to the tensile stress axis. Correspondingly, in wire-drawing which is closely akin to tension, a cylindrically symmetrical duplex *fibre texture* results which has *both* $\langle 111\rangle$ and $\langle 100\rangle$ parallel to the wire axis.

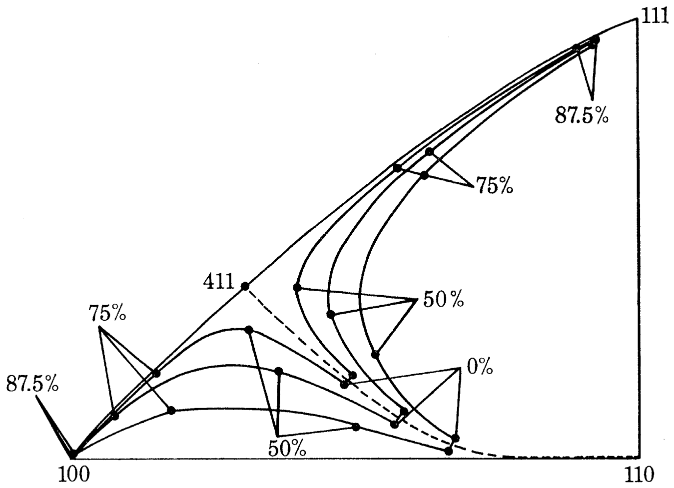

FIGURE 3. Slip rotation paths for axisymmetric compressive deformation of a body-centred cubic metal, deforming by pencil glide. Three different initial orientations are indicated, with rotations corresponding to various compressive strains for each initial orientation. (Dillamore & Katoh 1974.)

Taylor's model has generated a host of variants, of which the most mathematically satisfactory is that due to Bishop & Hill (1951). They were able to prove that Taylor's theory fufils Schmid's empirical yield criterion, derived from single crystal experiments: the resolved shear stress reaches the critical level for the 5 systems chosen by Taylor without reaching it for any of the other potential systems (except where pairs of systems happen to be equally favoured). As is pointed out by Chin (1969) in his particularly clear account of the Taylor theory and its descendants, most of the derivative versions do not satisfy the Schmid yield criterion. Taylor's (and Bishop & Hill's) theory presumes that each grain deforms as does the assemblage, i.e. strain continuity is preserved, but this then renders *stress* continuity impossible. Accordingly, it is to be expected that the strain in each grain is non-uniform to allow stress continuity across grain boundaries. This requires more than 5 slip systems to operate, each non-uniformly across the grain, which in turn implies variable orientations in different parts of the deformed grain. This, indeed, is observed experimentally (see example in figure 4, below). In spite of these ineradicable defects, the Taylor/Bishop & Hill theory gives a good approximation to the textures observed in a variety of deformed aggregates.

Figure 3 shows a theoretical diagram constructed by Dillamore & Katoh (1974) which predicts, on the basis of the Taylor theory, how various starting orientations will rotate in a polycrystalline assemblage of iron crystals subject to compression. Iron deforms by so-called *pencil glide* slip along a rigidly defined direction, ⟨111⟩, but on a number of alternative planes. The same predicted polarization into two alternative end-orientations is evident. In fact, individual grains are apt to split into irregularly shaped regions, called *deformation bands*, which strive towards different orientational destinations. Barrett & Levenson (1940), in a now classic study, were the first to reveal such bands. (The terminology of these bands is today in a confused state, with several rival usages.) The use of the Kossel X-ray diffraction technique (Ferran, Doherty & Cahn 1971) allows the orientation to be rapidly mapped at many points of a single deformed grain, and when this technique is applied to grains in a moderately deformed iron polycrystal, results such as those in figure 4 are found (Inokuti & Doherty 1977 *a*, *b*). The lattice rotation is very variable indeed; the maximum rotation is much greater than would be expected for 40% strain according to the theoretical stereogram, figure 3, and the grain splits into deformation bands. (The high orientational spread of deformed grains is, as explained above, an expected departure from Taylor's simple model.) The trend of figure 3 is, however, qualitatively correct, and this applies generally to similar predictions based on a combination of the Taylor theory and slip systems of known crystallographic nature. It is easier to interpet wire-drawing (roughly equivalent to simple tension) and simple compression than it is to deal with rolling of sheets, since this is a more complex deformation mode. Similar interpretations have been attempted for much more complex processes. The most involved is Calnan & Clews's (1952) interpretation of the rolling texture of uranium, which has orthorhombic symmetry; this metal undergoes copious twin-gliding according to several distinct twinning laws, and this plays a major part in determining the rolling texture. Agreement between theory and experiment is only moderately good.

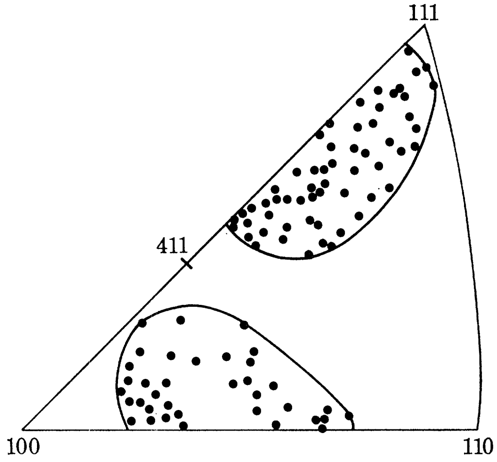

FIGURE 4. Orientations of various positions in a single grain of polycrystalline iron deformed 40% in compression. Orientations were determined by individual X-ray Kossel diffraction photographs. The two groups of orientations correspond to the matrix and to a series of deformation bands. (Inokuti & Doherty 1977 *b*.)

The detailed interpretation even of the supposedly simple wire textures is, in fact, a good deal more subtle than at first appears. Figure 5 (English & Chin 1965) illustrates this point. It shows that the relative proportions of ⟨111⟩ and ⟨100⟩ fibre textures in drawn wires in a number of different face-centred cubic metals and solid solutions varies as a function of the normalized energy of a stacking-fault (s.f.e.) (where the stacking of successive close-packed planes is locally anomalous). The value of the s.f.e. determines the fine structure of the individual dislocations in these materials, and this in turn governs the details of the slip morphology (e.g. 'cross-slip' on rogue {111} planes) and also determines how rapidly the latent (potential) slip systems, which do not actually operate, themselves work-harden. Finally, and most important, the s.f.e. determines the ease of twin-gliding (deformation-twinning in metallurgical parlance). Chin (1969) explains in detail how these various factors can be used to interpret figure 5. In particular, the almost pure ⟨100⟩ texture of drawn silver wire can be firmly attributed to the intermediate ease of twinning in this metal when intensely deformed (Ahlborn & Wassermann 1963). At still smaller stacking fault energies, twinning becomes so easy relative to slip that the pattern of lattice rotations changes again. For further particulars, Chin's paper must be consulted. Generally, the rôle of twinning in contributing to reorientation of a single crystal is quite involved, because the orientation dependence of the stress required to initiate twinning is itself a function of stacking-fault energy (Narita & Takamura 1974).

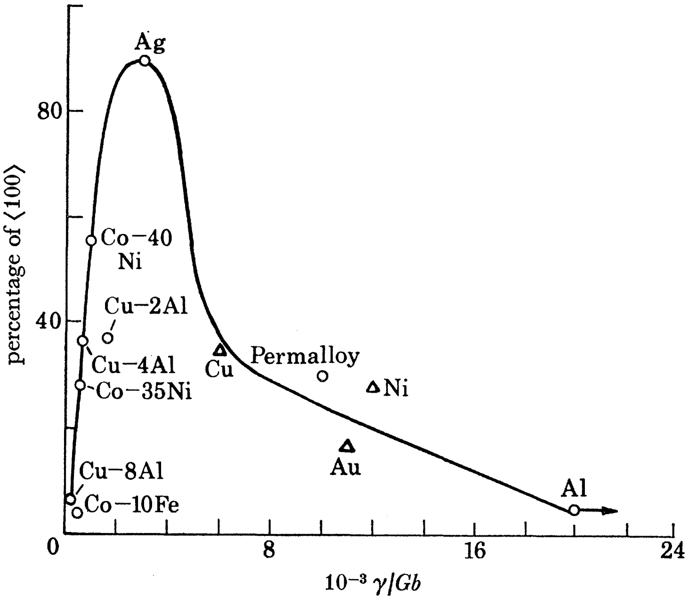

FIGURE 5. The variation of the proportions of ⟨111⟩ and ⟨100⟩ textures in duplex wire textures of face-centred cubic metals as a function of the specific stacking-fault energy parameter γ/Gb, where γ is the stacking fault energy, G is the shear modulus and b the magnitude of the Burgers vector. (English & Chin 1965.)

The details of rolling textures of the various families of metals are far too involved even to summarize here, as are the rival theories advanced to interpret them. An excellent outline will be found in Barrett & Massalski's book (1966), and a fuller account in the survey by Hu, Cline & Goodman (1966). The most thoroughly studied feature is the transition, in face-centred cubic metals and alloys, from a (123) $[\bar{4}\bar{1}2]$ ideal texture to a (110) $[\bar{1}12]$ ideal texture (both shown in figure 1) as a result of extensive alloying; lowering the rolling temperature also plays a part. This transition is again linked to the specific stacking-fault energy, which is plainly a major determinant of textures of all kinds in face-centred cubic metals and alloys.

3. Cold and hot deformation of textured sheets

The control of texture in sheets has become a major industrial necessity, primarily because of the widespread use of the deep drawing process. This is illustrated in figure 6. The extent of deformation possible in drawing is intimately related to the mechanical anisotropy of the sheet, and this in turn is linked to the nature and sharpness of the texture. The preferred measure of mechanical anisotropy is the *R-value* defined as ϵ_w/ϵ_t; ϵ_w, ϵ_t are width and thickness strains, respectively, in a sheet plastically deformed in uniaxial tension. For isotropic (texture-free) material, $R = 1$, while the extent of anisotropy in a textured sheet is best measured by $\bar{R}$, which is the mean of R-values averaged for all possible tensile directions in the plane of the sheet. Figure 7 shows that deep-drawability is enhanced by a high $\bar{R}$-value, and figure 8 in turn

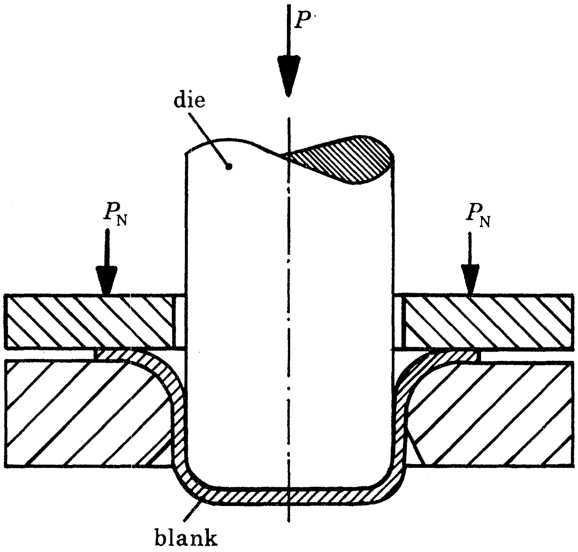

FIGURE 6. Arrangement for deep drawing of a circular sheet-blank.

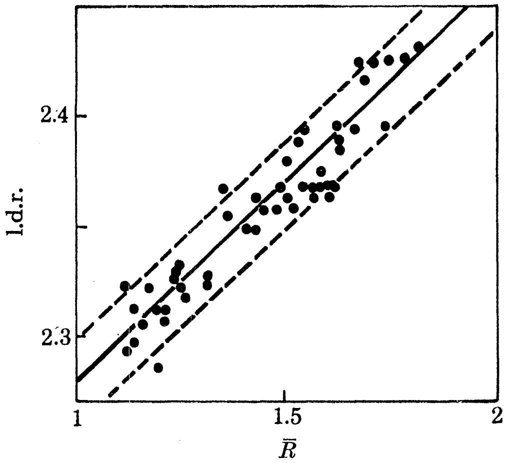

FIGURE 7. The dependence of deep drawability of mild steel, represented by the limiting drawing ratio (l.d.r. = ratio of the diameter of the largest blank which can be completely drawn without fracture to the diameter of the punch) as a function of the average R-value for the material. (Atkinson & McLean 1965.)

shows how the $\bar{R}$-value of a steel sheet is determined by texture. A high $\bar{R}$-value implies a good resistance to sheet-thinning, and it can be shown from macroscopic plasticity theory (Panknin 1969) that under these circumstances a larger drawing strain is feasible before the fracture stress is reached in the most thinned part of the drawn disk.

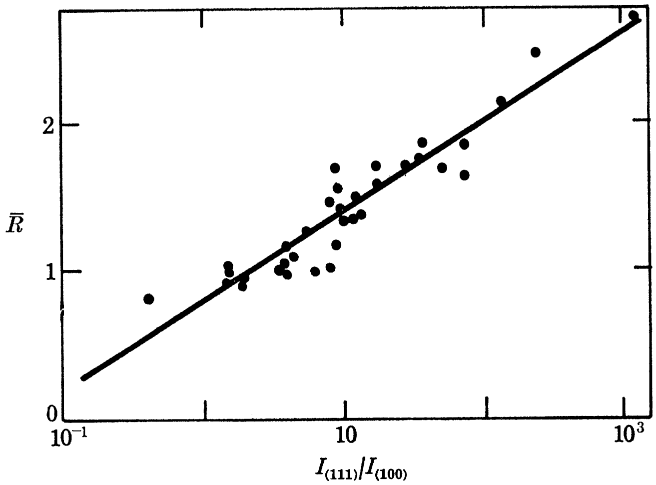

Figure 8. Average $\bar{R}$-value of mild steel as a function of the volume ratio of grains having (111) and (100) parallel to the sheet plane (I_{111}/I_{100}). (Held 1967.)

Conversely, it is possible to strengthen sheets by judicious choice of texture: this applies especially to metals of hexagonal symmetry such as titanium, which have a smaller number of alternative slip systems than do cubic metals. The successful practice of *texture-strengthening* requires a subtle understanding of macroscopic plasticity and the rôle of anisotropy, and ideally requires an ability to calculate $\bar{R}$-values from known textures. This industrially important topic is outlined by Hosford (1969). Particular applications are exemplified by Chin, Hart & Wonsiewicz (1969; spring material) or by Babel & Frederick (1968; titanium sheet).

In contrast to the very extensive work on the influence of texture on the ductility and strength of sheets deformed at ambient temperature, almost nothing has been done to investigate the resistance to creep of textured materials. In view of the practical importance of creep, this is a remarkable omission. The rôle of grain *size* has been very extensively examined over the years (review by Langdon & Mohamed 1975) and it is now recognized that, except for the smallest grain sizes, where grain-boundary shear begins to dominate, this factor plays a much smaller rôle than formerly believed. The only systematic attempt to examine the rôle of texture on creep was made by Barrett, Lytton & Sherby (1967). They examined steady-state creep in pure copper as a function of grain size for randomly orientated metal and as a function of texture – (100)[001] or random – at constant grain size (0.03 mm). The grain-size effect was appreciable only for grain diameters smaller than 0.2 mm, and was attributed primarily to a sensitivity of the incidence of grain-boundary shear to grain size at small grain sizes only. The replacement of random sheet by intensely textured sheet reduced the creep rate at all stresses by a factor of only two. The reduction was attributed to the exclusion of grain-boundary shear in the textured material.

There is need for further investigation, in a range of metals, especially non-cubic, of the rôle of texture in conferring resistance to creep.

4. ANNEALING TEXTURES

If a drawn wire or rolled sheet has been deformed substantially enough to generate a pronounced deformation texture, then on subsequent annealing it will always be found to have a pronounced annealing texture. Recrystallization does not generate random orientations, and indeed texture-free annealed sheets are difficult to make. The texture is often quite distinct, in a crystallographic sense, from the original deformation texture, and its nature can be affected by annealing temperature and time and even by the nature of the atmosphere. The annealing textures are not determined by the deformation texture alone: for instance, the addition of a modest amount of solute may sharply alter the annealing texture without creating any detectable changes in the prior deformation texture. Nevertheless, since all the 'genetic' information leading to the annealing texture must be present in the deformation texture, a change in one implies some change in the other, even if undetectable. Thus two sheets giving the same pole figure may have a different spatial distribution of the texture constituents. The theoretical problem is to understand how the 'genes' do their work or – to change the metaphor – how 'memory' is transmitted from deformed to recrystallized structure.

There is no need to go into details of particular textures; a very full account was published by Grewen & Wassermann (1962) and a more concise outline by Barrett & Massalski (1966). Of the many surveys dealing with the mechanisms of annealing texture formation, one which is particularly comprehensive and clear is that by Hutchinson (1974). The underlying mechanisms of recrystallization have been surveyed by Cahn (1970).

For many years, the theory of texture formation was characterized by a conflict between two extreme views – the *orientated nucleation* and *orientated growth* hypotheses. The former view is based on the central principle that new recrystallized grains generated by annealing a deformed structure have orientations which were present in the latter – that is, the nuclei are present all along, and annealing merely activates their growth. (It is reminiscent of the aesthetic dogma that a sculpture is latent in the raw block of marble.) On this hypothesis, textures are determined by what orientations are available. On the orientated growth hypothesis in its pure form, when a deformed metal is annealed all orientations are generated with equal probability at the nucleation stage. This evidently presupposes a nucleation mechanism different from that outlined above. Some nuclei then *grow* faster than others because of the restraining effect of the deformation texture on some of the growing grains. If a new grain is favourably orientated with respect to all or most components of the deformation texture, it will grow apace.

The orientated growth theory is buttressed by a body of experimental information which establishes that the growth rate of a strain-free grain into a dislocated grain is a function of mutual orientation, especially in the presence of small amounts of solutes which are believed to segregate to the grain boundary. These experiments have the limitation that the deformed grains used all had very low dislocation densities. The experiments have been surveyed by Aust (1969) and the corresponding theory of impurity-limited grain boundary migration by Gordon & Vandermeer (1966).

The orientated nucleation theory is buttressed by a growing body of microstructural investigation of the early stages of recrystallization which has established that nuclei do indeed grow from pre-existing orientations. This has been established particularly by the technique of Kossel X-ray diffraction, which allows the orientations of small new grains to be related to the local orientation of the deformed parent grain nearby. (It is essential to know the *local* orientation of a deformed grain, because overall such a grain has a surprisingly wide orientation range.) This technique has been applied to aluminium (Ferran *et al.* 1971; Doherty & Cahn 1972; Bellier & Doherty 1977) and iron (Inokuti & Doherty 1977*a*, *b*). In both metals, deformed in the range 20–40 % reduction, it is unambiguously clear that new grains grow from preexisting orientations at locations where there is a steep orientation gradient: this implies either intergranular boundaries or the narrow *transition bands* between adjacent deformation bands within individual grains. (These bands might be described as 'artificial grain boundaries', with very large misorientations.) At smaller strains, nucleation was preferentially at true grain boundaries; at larger strains, 'artificial grain boundaries' were preferred. The physical process involved in the nucleation is *strain-induced boundary migration*; a deformed grain or deformation band bulges into its neighbour, achieving a low dislocation density as it does so. The early stages of this well-documented process have been analysed by Doherty & Cahn (1972) and the energy balances which govern the process were originally examined by Bailey (1960) and more comprehensively (in connection with the special problem of nucleation at transition bands) by Dillamore, Morris, Smith & Hutchinson (1972).

In the past, attempts to interpet annealing textures were based on analysis of pole figures 'before and after', with attempts either to verify that the two major texture components of the annealing texture were present in the deformation texture (to support orientated nucleation) or to show that appropriate components of the two textures were related in such a way as to favour rapid growth (to support orientated growth). This is a blunt approach which can be sharpened by recourse to the more sophisticated orientation distributions (see above) to replace ordinary pole figures. This has been done recently with regard to textures in copper and its alloys (Schmidt, Lücke & Pospiech 1974). The conclusion is that in general there is an element of growth selection operating on a non-random supply of available nuclei, themselves the product of orientated nucleation. There are particular textures the origin of which is still debated, and chief among these is the peculiar 'cube texture', (100) [001], in copper and its alloys. Small composition changes which do not detectably change the deformation texture (R. K. Kay, quoted by Hutchinson 1974) completely alter the annealing texture. The orientated growth and nucleation theories have alternately held the field and, as Hutchinson shows, this debate continues apace.

Orientated nucleation – with its concomitant element of growth selection – is only part of the story. It is becoming plain that different components of a deformation texture may have differing proclivities to nucleate new grains on annealing. Dillamore, Smith & Watson (1967) were the first to establish, by electron microscopy, that in iron the stored energy of various grains in a rolled sheet increases in the sequence $(100)[011]$, $(211)[0\bar{1}1]$, $(111)[uvw]$, $(011)[0\bar{1}1]$. (The last is a very minor component.) The stored energy increases with the average strain needed to bring randomly orientated initial grains into the particular orientation under consideration. The most highly deformed texture components will recrystallize first, and any processing variable which delays nucleation gives the first-comers more time to grow. This will sharpen the annealing texture and (in the case of iron) enhance the (111) component which is in fact desired for its high $\bar{R}$ value and good drawability. Precise control of precipitates such as AlN, NbC and Cu has this desirable effect. The complex balance of variables involved has been ably reviewed by Hutchinson (1974) and, in somewhat greater detail, by Hatherly & Dillamore (1975).

Annealing textures may alter even after recrystallization is complete, during the subsequent stage of grain growth. There are two entirely distinct forms of grain growth: *normal* grain growth leads to a gradual *uniform* increase in size of surviving grains, while *abnormal* grain growth (secondary recrystallization, coarsening) involves extreme growth of a few grains and stasis of all others. Surprisingly, almost no research has been done on textural changes during *normal* grain growth. Dunn & Walter (1966) explain why only normal grain growth would be expected to remove grains furthest from the average texture, and thus sharpen the texture. Rauch, Thornberg & Foster (1977) have very recently established that precisely this happens in low-alloyed iron: the (110)[001] texture is sharpened during normal grain growth.

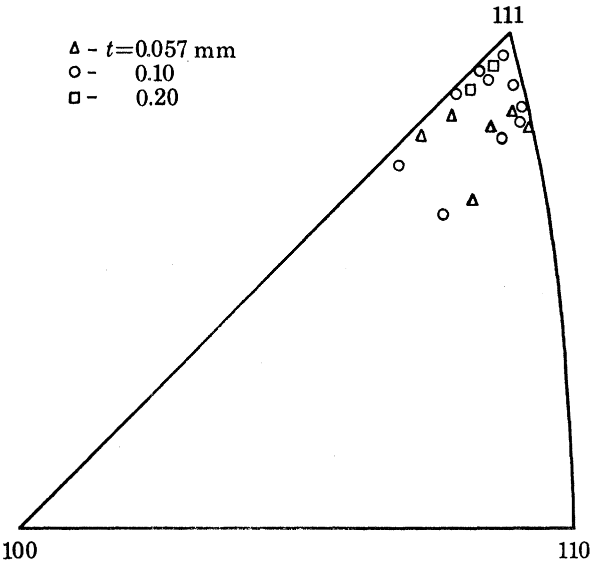

FIGURE 9. Poles of planes parallel to the free surface of individual secondary grains in sheets of high-purity platinum of three different sheet thicknesses, after annealing at 1500 °C. (McLean & Mykura 1965.) The factors governing the sharpness of the texture are discussed by Dunn & Walter (1966).

Secondary recrystallization, however, has been copiously examined, and excellently reviewed by Dunn & Walter (1966) and Walter (1969). The selective growth of a few grains 'takes off' when these grains exceed the average size by a sufficient factor, between 2 and 3. This arises from a size-dependent inbalance of tensions at grain-boundary triple points. A variety of structural factors can bring a population of recrystallized grains to this 'take-off' condition': a sharp annealing texture with a few deviant grains, a critical dispersion of precipitates which will restrain most grains but not all, or anisotropy of surface energy. In all cases, the large grains which win the race have a pronounced texture which is generally quite different from the original annealing texture. The production of the celebrated 'Goss texture' in iron–silicon alloys, (110)[001], which confers superior magnetic properties on transformer laminations and is of major industrial importance, is generated by secondary recrystallization controlled through subtle manipulation of dispersed precipitates.

A particularly interesting form of texture generation during secondary recrystallization is associated with surface energies. Thus, thin sheets of platinum (McLean & Mykura 1965) will develop large secondary grains all with (111) closely parallel to the surface (figure 9).

This happens because this orientation has a particularly low surface energy. An even more remarkable variant of this behaviour is the change of texture which results from changing the composition of the atmosphere in which an iron–silicon alloy is annealed: (110) parallel to the surface is favoured *in vacuo* and (100) in oxygen-bearing argon. Hydrogen containing H_2S favours (100). The very complex factors determining relative surface energies of different orientation as a function of atmosphere are fully analysed by Dunn & Walter (1966). They also show that for such surface energy factors to play a major rôle, the sheet has to be thin and the grain size large, because only in this way is the driving force associated with surface energy large enough to outweigh other driving forces associated with grain boundary energy and drag by precipitate particles. The matter of driving forces is one to which we shall return at the end of this review.

5. Textures in quartz and the rôle of Dauphiné twinning

In view of the geological importance of quartzite (polycrystalline quartz) and its possible rôle as an indicator of past tectonic processes, it is worthwhile, in the context of this Discussion, to compare the textural characteristics of quartzite with those of metals.

While quartzite is brittle at normal temperatures and pressures, it flows by dislocation movement readily when hot and under hydrostatic pressure, and especially if weakened by water. Hobbs (1968) has shown that single quartz crystals when deformed under such conditions in the laboratory and then annealed, recrystallize in much the same way as aluminium or iron, from nuclei forming at deformation band boundaries. (Hobbs calls them 'kink bands', adding further to the terminological luxuriance.) Optical analysis of *c* axis orientations shows that strain-induced boundary migration occurs here also. Similar behaviour has been reported in orthopyroxene (Etheridge 1975). White (1976) has recently examined, by electron and optical microscopy, the deformation and recrystallization of quartzite and has found that nucleation at grain boundaries (mantles) also occurs as in metals. White's paper shows a comprehensive familiarity with the metallurgical literature and the resemblances between quartzite and polycrystalline metals are firmly established. The textures (fabrics) formed in quartzite appear to be generated similarly to those in metals, though the experimental information is much sparser. In particular, polarized-light techniques as normally used in the examination of quartzite fabrics reveal the orientation of the *c* axis only and do not permit the construction of a complete pole figure, let alone orientation distributions. This would require X-ray diffraction which does not seem to be much used in this field of study.

An exception to this rule is found in the particularly important textural studies of Tullis (1970) and Tullis & Tullis (1972). They hot-deformed quartzite by uniaxial compression under superimposed large hydrostatic pressure to render the rock plastic. They used standard X-ray methods to obtain inverse pole figures such as figure 10*a*, and present persuasive evidence that the texture revealed in such pole figures is primarily due *not* to plastic deformation by dislocation mechanisms or indeed to normal recrystallization mechanisms but to the unfamiliar process of *Dauphiné twinning*.

Low or α-quartz, crystal class 32, is subject to several distinct forms of twin, of which one, the Dauphiné twin, is generated by a 180° rotation of the lattice about the threefold axis. The resultant rearrangement of the crystal structure is shown in figure 11. The Dauphiné twin is the prototype of what Klassen-Neklyudova, in her review of mechanically induced twinning (1964), calls 'twinning without change of form'. It is *not* a shear-twin, formed by twin gliding like the familiar lamellar twins in iron, zinc or uranium, but instead involves only atom shifts small compared with interatomic separations. (In M. J. Buerger's well-known terminology, Dauphiné twinning is *displacive* as distinct from the *reconstructive* process involved in twin-gliding.) In natural quartz crystals, Dauphiné twins occur as complex intergrowths. Tsinzerling was the first to observe that Dauphiné twin configurations could be generated by sustained application of concentrated loads on various faces of twin-free crystals, most easily at high temperatures; details may be found in Klassen-Neklyudova's book. Figure 12 summarizes the morphology of these pressure-induced twins, which are generated the more easily, the higher the temperature. Subsequent experimenters (Wooster, Wooster, Rycroft & Thomas 1947; Thomas & Wooster 1951; Aizu 1973; Newnham, Miller, Cross & Cline 1975) have established that the twin interface (probably controlled by a distribution of ultrafine precipitate particles) will move under an effective stress of *ca.* 50 kgf/mm^2 at room temperature, reducing to 0.1–1.0 kgf/mm^2 at 400–500 °C. (At 573 °C, α-quartz transforms into hexagonal β-quartz, and this is not subject to Dauphiné twinning.) The twin interface tends to be plane (Aizu 1970; Newnham & Cross 1974) but easily breaks away to adopt an arbitrary configuration like an ordinary grain boundary. (In fact, it is helpful to regard complex Dauphiné twin configurations as though they were grain configurations involving two fixed orientations only.)

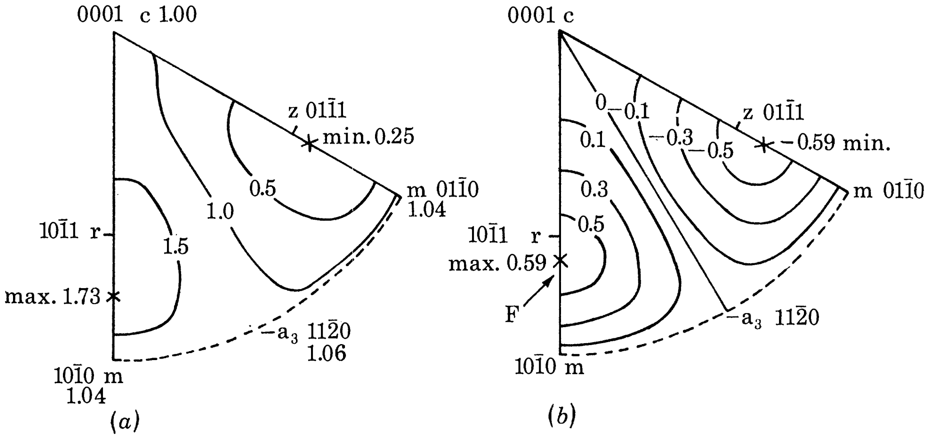

FIGURE 10. (*a*) *Inverse* pole figure for a flint (fine-grained form of quartzite) loaded at 500 °C and a confining pressure of 4 kbar to a differential compressive stress of 13 kbar for 3 h. The pole figure shows the distribution of the stress direction, and contours are in multiples of a uniform (random) distribution. (*b*) *Inverse* pole figure showing the variation with crystal direction in α-quartz of the *difference* in S'_{11} between original and twinned orientations, in units of 10^{-12} cm^2/dyn. Equal-area projections are used as distinct from conventional stereographic projections. (Tullis 1970.)

Since Dauphiné twins do not form by shear, how does it come about that an applied stress can create and cause to grow a twin-orientated region? Thomas & Wooster (1951), in a classic study, answered this question when they discovered that if a particular applied stress-pattern was able to move a twin boundary, then the same stress pattern with signs of all stresses reversed would move the twin boundary in the *same* direction as before. This implies that the important factor is the square of the stresses, and this led Thomas & Wooster to the recognition that the crucial factor was the stored elastic energy, which involves the squares of the applied stresses. The twinned domains grow or contract in such a way that, in the end result, *the whole crystal yields elastically as much as possible under a given stress*. This is simply a corollary of the Le Chatelier principle. Many subsequent investigators have examined this criterion both experimentally and theoretically (see Paterson 1973 for a critical survey) and it is now well established for the case of constant applied stress. (For the special case of constant applied *strain*, it does not apply; see Tullis & Tullis 1972.) Because domains grow under applied stress, Thomas & Wooster coined the name *piezocrescence* for the process, but this expressive term does not seem to have been widely adopted.

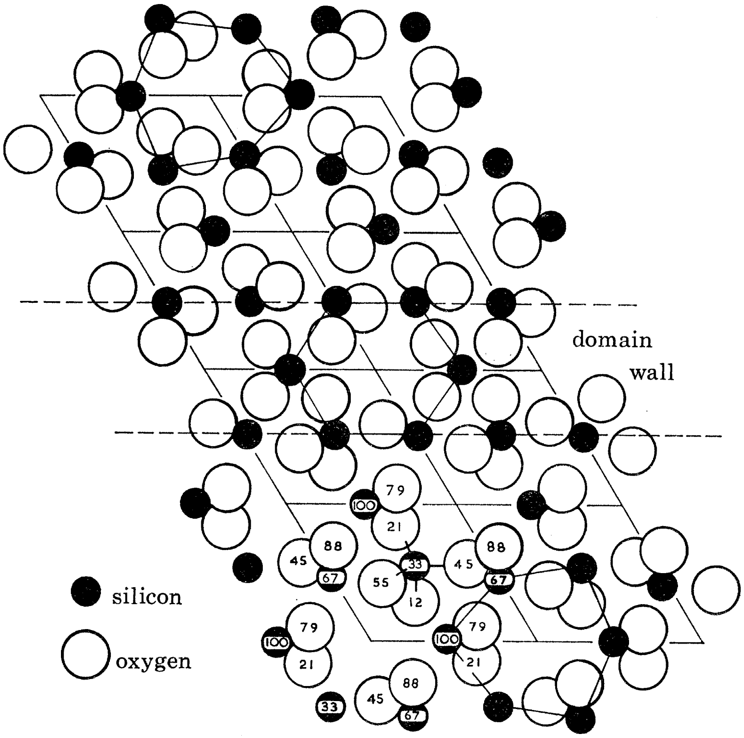

FIGURE 11. c-axis projection of the structure in both parts of a Dauphiné twin in α-quartz. One SiO_4 tetrahedron (atoms 12, 21, 33, 45, 55) is shown bonded. The numbers are atomic heights expressed as fractions of 100. The figure indicates how small are the displacive shifts required to permit the domain wall to move and one orientation to grow at the expense of the other. (Anderson *et al.* 1976.)

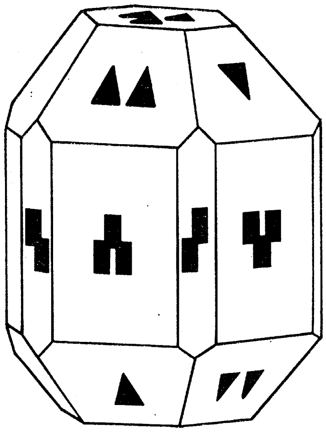

FIGURE 12. Surface traces of Dauphiné twins on the principal faces of a α-quartz crystal, generated by concentrated normal loading for prolonged periods. All Dauphiné twins have the same orientation. (Tsinzerling, as reproduced by Klassen-Neklyudova 1964.)

Dauphiné twinning in quartz is a special case of what has recently been recognized (Aizu 1970, 1973) as *ferroic* behaviour in a variety of crystals which can be transformed from one bistable state to the other by applied stress, magnetic or electric field, or combinations of these. The very involved physics and crystallography of the family of ferroic crystals is very clearly outlined by Newnham (1975).

For the simple case of uniaxial compression under superimposed hydrostatic pressure, the driving force ΔW causing a Dauphiné twin boundary to move is given by $\Delta W = \frac{1}{2}\Delta S'_{11}\,\sigma^2$, where σ is the (differential) compressive stress, S'_{11} is the reciprocal of Young's modulus (i.e. the elastic compliance) in the direction of the applied stress and $\Delta S'_{11}$ is the difference in the value of S'_{11} in the two constituent orientations of the twin. ΔW measures the difference in stored elastic energy for the two extremes of a crystal consisting entirely of one twin orientation or entirely of the other. ΔW has the dimensions of energy per unit volume or force per unit area (Tullis & Tullis 1972). If the stress system is more complicated, then a complex tensor criterion takes the place of the simple Tullis criterion (Newnham 1975; Anderson, Newnham, Cross & Laughner 1976). The considerable interest by physicists in this topic stems from the importance of quartz slices as oscillators in electrical circuits. Formerly (Wooster *et al.* 1947) the overriding aim was to remove all twins, but now it has been recognized that controlled twin configurations, generated by local laser-heating, can remove unwanted harmonics and improve oscillator performance (Newnham *et al.* 1975; Anderson *et al.* 1976).

The general concept of a driving force – or, more exactly, the force on an interface – has been examined by Eshelby (1970).

Tullis & Tullis uniaxially compressed randomly orientated fine-grained quartzites or flints at elevated temperatures under a confining pressure to make plastic deformation possible. Figure 10*a*, an *inverse* pole figure, shows the distribution of the stressing axis relative to the α-quartz unit cell for a flint loaded at 500 °C and a confining pressure of 4 kbar† to a differential compressive strain of 13 kbar (*ca.* 130 kgf/mm²). In figure 10*b*, values of $\Delta S'_{11}$ are shown for the same range of compression axes. It can be seen that the two pole figures are quite similar, which is a clear indication that the texture was formed by stress-induced Dauphiné twinning, i.e. that the more compliant directions tend, statistically, to be aligned with the stress. Whether this should be called a deformation texture or an annealing texture is a moot question: perhaps 'dynamic annealing texture' would best meet the circumstances of its genesis.

Tullis (1970) and Tullis & Tullis (1972) systematically varied the temperature and differential compressive stress and also used quartzites and flints with different impurity contents, and examined the resultant textures. (They established a simple statistical test to determine the contribution of factors other than Dauphiné twinning to texture formation. In all instances where a texture formed, it was found to be primarily due to twinning; a conventional deformation texture would generate a concentration of stress-axes near the centre of the pole figure (a '*c*-axis texture'), and thus a mixture of Dauphiné texture and conventional deformation texture causes a shift of the 'maximum' position from *F* nearer to the *c*-axis.) The experimental findings can be summarized as follows:

(1) A sample such as that of figure 10*a*, showing only a very small permanent strain (no exact figures were quoted), had a texture entirely due to Dauphiné twinning. A substantial plastic strain (30–50 %) led to contributions from a *c*-axis texture, but even then the Dauphiné contribution remained strong.

---

† 1 kbar = 10^8Pa.

(2) For small strains, increasing the temperature at constant compressive stress led to stronger Dauphiné texture, up to a limiting temperature beyond which no further changes were found. This limiting temperature was much lower for purer quartzites, which confirmed that twin boundaries are constrained by impurities: the effect of temperature is essentially to provide thermal activation to overcome the twinning action of impurities. Finer-grained rocks (flints) formed stronger textures than coarse-grained quartzites, other things being equal.

(3) For small strains and constant temperature and purity, increasing stress leads to stronger Dauphiné texture. A large increase of stress is needed to achieve a modest increase of texture, i.e. texture intensity is not proportional to ΔW.

(4) Some samples which were deformed to substantial plastic strains had undergone dynamic recrystallization, others had not. In both cases there was a strong Dauphiné texture component, i.e. the Dauphiné twinning pattern can be repeatedly created after successive waves of dynamic recrystallization.

It follows from these observations that Dauphiné twinning, controlled by the elastic strain energy criterion, to a substantial extent controls texture in stressed quartzites and flints, *even in the absence of permanent strain.* In this last respect, these textures are different from anything known in metals. Tullis & Tullis (1972) conclude tentatively that Dauphiné textures offer scope for the assessment of the deformation history of naturally occurring quartz-rich rocks. It would be interesting to know whether very intense plastic deformation, as in mylonite zones in quartzites, proves to cause *c*-axis textures strong enough to swamp the Dauphiné component.

Driving forces

To a metallurgist, it is surprising that even in the presence of large plastic strains, the elastic strain criterion can nevertheless control a major component of the resultant texture. To conclude this section, therefore, we shall address this question by estimating the driving force for Dauphiné twin-texturing and comparing it with typical driving forces for recrystallization into a plastically deformed material. We will undertake the former calculation for a typical condition used by Tullis & Tullis, namely 15 kbar (differential) uniaxial stress. This is just enough to produce substantial permanent strain over a period of some hours at *ca.* 500 °C.

$\Delta S'_{11}$ (in the expression $\Delta W = \frac{1}{2}\Delta S'_{11}\,\sigma^2$) will be taken as the value for the most favourably orientated grain (position F in figure 10*b*). On this basis (compare figure 10*b*),

$$\Delta S'_{11} = 0.5\times 10^{-12}\ \mathrm{cm^2/dyn}, \quad \sigma = 15\ \mathrm{kbar} \approx 150\ \mathrm{kgf/mm^2} \approx 15\times 10^9\ \mathrm{dyn/cm^2},$$

whence

$$\Delta W \approx 5\times 10^7\ \mathrm{dyn/cm^2} \quad \text{or} \quad 5\ \mathrm{J/cm^3}.$$

In terms of a gram-molecular mass, the driving energy ≈ 130 J/mol. This surprisingly high driving force is directly attributable to the very high differential stress needed to deform quartzite plastically even at a temperature as high as 500 °C. No measurements are available of the stored energy of plastic deformation in quartzite, so we must take metallurgical data for comparison (see Martin & Doherty 1976). Thus copper, deformed to a logarithmic strain of 1.2, has a stored energy (= driving force for primary recrystallization) of *ca.* 50 J/mol. The maximum strain imposed in Tullis & Tullis's experiments was much less than this, so that one can conclude with confidence, even allowing for the unknown differences between copper and quartz, that the driving force for Dauphiné-twinning is somewhat greater than that for conventional recrystallization of plastically deformed rock. We can now understand why a strong Dauphiné texture forms even in permanently deformed and recrystallized quartzites.

For comparison, the following are representative driving forces for other microstructural processes: a phase change, such as the precipitation of $CuAl_2$ from an Al–Cu solid solution at 600 K; 1200 J/mol. The driving force for normal grain growth, in a metal of grain diameter 0.03 mm and boundary energy of 0.5 J/m^2, is only about 0.5 J/mol. This is the energy liberated by complete elimination of the boundaries. For secondary recrystallization controlled by differential surface free energy (for an iron sheet 0.1 mm thick, an initial grain size of 1 mm, a surface energy ratio of $\sigma_{100}/\sigma_{110} = 0.9$ and $\sigma_{100} \approx 2.1$ J/m^2), the driving force $\approx 3 \times 10^{-2}$ J/mol. It is thus not surprising that this effect is found only after primary recrystallization is complete: if any appreciable plastic deformation were to remain, the stored energy associated with the dislocations would utterly swamp the frail driving force favouring (100)-orientated grains over (110)-orientated grains! The driving force associated with a magnetic field applied to a ferromagnetic polycrystalline sheet leading in principle to the selection of grains with a particularly high induction, is smaller still, and indeed there is no convincing evidence that a magnetic field can affect the annealing texture of a steel. The directed migration of a grain boundary in a (diamagnetic) bismuth bicrystal under the influence of a very large magnetic field has been recorded (Mullins 1956) but there is no record of any influence on a texture.

It might have been supposed that elastic anisotropy might be able to generate an annealing texture in a highly anisotropic metal during grain growth following primary recrystallization, if a small stress (too small to cause creep) were to be applied during the anneal. Thus for zinc, the largest value of $\Delta S'_{11}$ would be $S_{33} - S_{11}$, about 2×10^{-12} cm^2/dyn (larger than ΔS for quartz). A typical flow stress at ambient temperature for polycrystalline zinc is 25 kg/mm^2; if a compressive stress of one quarter of this value were applied at say 250 °C, then $\Delta W = \frac{1}{2}\Delta S'_{11}\,\sigma^2$ would be about 1.5 J/mol, and grain growth should proceed under this directing influence. This value of ΔW is a much smaller value than we have found for quartz (because the stress is necessarily so small), but it exceeds the driving force for normal grain growth and in the absence of any plastic deformation to swamp the driving force, it should be quite sufficient to generate a texture by selection of favourably orientated grain during grain growth. This kind of texture in metals remains to be established.

I am grateful to Dr R. D. Doherty and Dr Y. Inokuti for allowing me to reproduce a stereogram from their work in advance of publication, and to Prof. R. E. Newnham for information about his research in advance of publication.

REFERENCES (Cahn)

Ahlborn, H. & Wassermann, G. 1963 *Z. Metallk.* **54**, 1.
Aizu, K. 1970 *Phys. Rev.* B **2**, 754.
Aizu, K. 1973 *J. phys. Soc. Japan* **34**, 121.
Anderson, T. L., Newnham, R. E., Cross, L. E. & Laughner, J. W. 1976 *Phys. Stat. Sol.* (a) **37**, 235.
Atkinson, M. & McLean, I. M. 1965 *Sheet Metal Industries* **42**, 290.
Aust, K. T. 1969 In *Textures in research and practice* (eds J. Grewen & G. Wassermann), p. 24. Berlin: Springer-Verlag.
Babel, H. W. & Frederick, S. F. 1968 *J. of Metals* (A.I.M.E.), October, p. 32.
Bailey, J. E. 1960 *Phil. Mag.* **5**, 833.
Barrett, C. R., Lytton, J. L. & Sherby, O. D. 1967 *Trans. met. Soc. Am. Inst. min. metall. Engrs* **239**, 170.
Barrett, C. S. & Levenson, L. H. 1940 *Trans. Am. Inst. min. metall. Engrs* **137**, 112.
Barrett, C. S. & Massalski, T. B. 1966 *Structure of metals*, 3rd edn, chs 20, 21. New York: McGraw-Hill.
Bellier, S. P. & Doherty, R. D. 1977 *Acta metall.* **25**, 521.
Bishop, J. F. W. & Hill, R. 1951 *Phil. Mag.* **42**, 414, 1298.

Bunge, H. J. 1965 *Z. Metallk.* **56**, 872.

Bunge, H. J. 1969 In *Textures in research and practice* (eds J. Grewen & G. Wassermann), p. 24. Berlin: Springer-Verlag.

Cahn, R. W. 1970 *Physical Metallurgy*, 2nd edn, ch. 19. Amsterdam: North-Holland.

Calnan, E. A. & Clews, C. J. B. 1952 *Phil. Mag.* **43**, 93.

Chin, G. Y. 1969 In *Textures in research and practice* (eds J. Grewen & G. Wassermann), p. 51. Berlin: Springer-Verlag.

Chin, G. Y., Hart, R. R. & Wonsiewicz, B. C. 1969 *Trans. met. Soc. Am. Inst. min. metall. Engrs* **245**, 1669.

Davies, G. J., Dillamore, I. L., Hudd, R. C. & Kallend, J. S. (eds) 1975 *Texture and the properties of materials.* London: The Metals Society.

Dillamore, I. L. & Katoh, H. 1974 *Met. Sci.* **8**, 21, 73.

Dillamore, I. L., Morris, P. L., Smith, C. J. E. & Hutchinson, W. B. 1972 *Proc. R. Soc. Lond.* A **329**, 405.

Dillamore, I. L., Smith, C. J. E. & Watson, T. W. 1967 *Met. Sci. J.* **1**, 49.

Doherty, R. D. & Cahn, R. W. 1972 *J. less-common Metals* **28**, 279.

Dunn, C. G. & Walter, J. L. 1966 In *Recrystallization, grain growth and textures* (ed. H. Margolin), p. 295. Metals Park: American Society for Metals.

English, A. T. & Chin, G. Y. 1965 *Acta metall.* **13**, 1013.

Eshelby, J. D. 1970 In *Inelastic behaviour of solids* (eds M. F. Kanninen *et al.*), p. 77. New York: McGraw-Hill.

Etheridge, M. A. 1975 *Tectonophysics* **25**, 87.

Ferran, G., Doherty, R. D. & Cahn, R. W. 1971 *Acta metall.* **19**, 1019.

Gordon, P. & Vandermeer, R. A. 1966 In *Recrystallization, grain growth and textures* (ed. H. Margolin), p. 205. Metals Park: American Society for Metals.

Grewen, J. & Wassermann, G. 1962 *Texturen metallischer Werkstoffe.* Berlin: Springer-Verlag.

Hatherly, M. & Dillamore, I. L. 1975 *J. Austral. Inst. Metals* **20**, 71.

Held, J. F. 1967 *Trans. met. Soc. Am. Inst. min. metall. Engrs* **239**, 573.

Hobbs, B. E. 1968 *Tectonophysics* **6**, 353.

Hosford, W. F. 1969 In *Textures in research and practice* (eds J. Grewen & G. Wasserman), p. 464. Berlin: Springer-Verlag.

Hu, Hsun & Goodman, S. R. 1963 *Trans. Am. Inst. min. metall. Engrs* **227**, 627.

Hu, Hsun, Cline, R. S. & Goodman, S. R. 1966 In *Recrystallization, grain growth and textures* (ed. H. Margolin), p. 295. Metals Park: American Society for Metals.

Hutchinson, W. B. 1974 *Met. Sci.* **8**, 185.

Inokuti, Y. & Doherty, R. D. 1977*a* *Textures crystall. Solids* **2**, 143.

Inokuti, Y. & Doherty, R. D. 1977*b* *Acta metall.* **25**. (In the press.)

Kalland, J. S. & Davies, G. J. 1972 *Phil. Mag.* **25**, 471.

Klassen-Neklyudova, M. V. 1964 *Mechanical twinning of crystals*, pp. 87, 150. New York: Consultants Bureau.

Langdon, T. G. & Mohamed, F. A. 1975 In *Grain boundaries in engineering materials* (*Proc. 4th Bolton Landing Conf.*) (eds J. C. Walter & J. H. Westbrook), p. 339. Baton Rouge: Claitor's Publishing Division.

McLean, M. & Mykura, H. 1965 *Acta metall.* **5**, 628.

Martin, J. W. & Doherty, R. D. 1976 *Stability of microstructure in metallic systems*, pp. 5, 82. Cambridge University Press.

Mullins, W. W. 1956 *Acta metall.* **4**, 421.

Narita, N. & Takamura, J. 1974 *Phil. Mag.* **29**, 1001.

Newnham, R. E. 1975 *Structure–property relations*, ch. 4. Berlin: Springer-Verlag.

Newnham, R. E. & Cross, L. E. 1974 *Mater. Res. Bull.* **9**, 1021.

Newnham, R. E., Miller, C. S., Cross, L. E. & Cline, T. W. 1975 *Phys. Stat. Sol.* (a) **32**, 69.

Panknin, W. 1969 In *Textures in research and practice* (eds J. Grewen & G. Wassermann), p. 464. Berlin: Springer-Verlag.

Paterson, M. S. 1973 *Rev. Geophys. & Space Phys.* **11**, 355.

Rauch, G. C., Thornburg, D. R. & Foster, K. 1977 *Metall. Trans.* **8 A**, 210.

Roe, R. J. 1965 *J. appl. Phys.* **36**, 2024.

Schmid, E. & Boas, W. 1935 *Kristallplastizität.* Berlin: Springer-Verlag.

Schmidt, W., Lücke, K. & Pospiech, J. 1974 In *Texture and the properties of materials* (eds G. J. Davies *et al.*), p. 147. London: The Metals Society.

Taylor, G. I. 1934 *J. Inst. Metals* **62**, 307.

Thomas, L. A. & Wooster, W. A. 1951 *Proc. R. Soc. Lond.* A **208**, 43.

Tullis, J. 1970 *Science, N.Y.* **168**, 1342.

Tullis, J. & Tullis, T. 1972 In *Flow and fracture of rocks*, Geophysical Monograph Series, no. 16 (eds H. C. Heard *et al.*), p. 67. Washington: American Geophysical Union.

Walter, J. L. 1969 In *Textures in research and practice* (eds J. Grewen & G. Wassermann), p. 227. Berlin: Springer-Verlag.

White, S. 1976 *Phil. Trans. R. Soc. Lond.* A **283**, 69.

Wooster, W. A., Wooster, N., Rycroft, J. L. & Thomas, L. A. 1947 *J. Instn Elect. Engrs* **94** (part IIIA), 927.